Thermochimica Acta, 213 (1993) 47–82
Elsevier Science Publishers B.V., Amsterdam

Effusion chemistry in the GaTe–Ga system

Pannee Mukdeeprom-Burckel and Jimmie G. Edwards

Department of Chemistry, The University of Toledo, Toledo, OH 43606 (USA)

(Received 6 April 1992)

Abstract

Gallium telluride is an important example for understanding the high temperature chemistry of III–VI phases. It is used in optical recording devices and a variety of thin-film ternary-phase applications. In this work, the vaporization chemistry and vapor pressure of Ga–Te samples with initial mole fractions of Te of 0.503 ± 0.002 and 0.436 ± 0.003 were studied in the temperature range 921–1102 K by the simultaneous Knudsen effusion and Volmer (torsion) effusion method. A new phase, $GaTe_{0.96\pm0.02}$(s), was discovered and modification to published phase diagrams of Ga–Te was made. Two quadruple points were observed: [liquid (L2) with 10 mol% Te, monotectic liquid (L1) with 30 mol% Te, $GaTe_{0.96\pm0.02}$(s), and vapor at 1029 ± 12 K and $0.22(+0.10/-0.09)$ Pa]; [(L2), $GaTe_{0.96\pm0.02}$(s), GaTe(s), and vapor at 968 ± 42 and $0.026(+0.094/-0.022)$ Pa]. Chemical analyses of starting materials and residues showed the effusion of GaTe(s) and $GaTe_{0.96\pm0.02}$(s) to be incongruent, but that of the latter is very close to being congruent. Vaporization reactions and their $\Delta H°(298\,K)$ were established in five composition and temperature ranges. On the basis that $\Delta H°(298\,K)$ of GaTe(s) and $\frac{1}{2}Te_2$(g) are -78.8 ± 2.4 and 84.2 ± 0.4 kJ mol^{-1}, respectively, then the $\Delta H°(298\,K)$ of GaTe(s) and $GaTe_{0.96\pm0.02}$(s) are -104 ± 15 and -101 ± 15 kJ mol^{-1}, respectively.

INTRODUCTION

This work is part of an effort to study the vaporization chemistry of a group of ternary semiconductor compounds of the type $A^{II}B_2^{III}C_4^{VI}$ (A^{II} is, for example, Pb or Cd, B^{III} is In or Ga, and C^{VI} is S, Se, or Te) and to better understand the thermodynamics and kinetics of effusion processes in general. We anticipate that the vaporization and effusion processes of the ternary phases will be related to those of their binary constituents. Inconsistencies and large uncertainties in reports of the thermodynamic properties and vapor pressure of GaTe(s) led us to reinvestigate the effusion chemistry of GaTe(s).

Correspondence to: J.G. Edwards, Department of Chemistry, The University of Toledo, Toledo, OH 43606, USA.

GaTe(s) is a substance of special interest because it presents a variety of optical spectra depending on the polarization direction of the exciting light [1–3]. It is used in optical recording memory devices [4].

The phase diagram of the gallium–tellurium system has been presented by Klemm and Vogel [5] from thermal analysis, by Newman et al. [6] from thermal analysis and direct observations of melting points under controlled tellurium pressure, and later by Wobst [7], Alapini et al. [8], and Blachnik and Irle [9], all from differential thermal analysis (DTA) and X-ray diffraction (XRD) studies. All investigators agree on the existence of GaTe(s) and Ga_2Te_3(s). GaTe(s) has a monoclinic [8, 10–15] structure and a metastable hexagonal structure which forms under strongly nonequilibrium conditions [10]. Ga_2Te_3(s) has a zinc blende structure [5, 6, 8, 10, 16, 17] and a superlattice structure which forms upon slowly cooling Ga_2Te_3 from 723 K [18]. Other phases at different compositions have been reported by various investigators. Newman et al. [6] have reported two high temperature phases, Ga_3Te_2(s) and $GaTe_3$(s), to be stable in the temperature ranges 883–1026 K and 681–702 K, respectively. $Ga_{2+x}Te_3$ has been found in thin films by Semiletov and Vlasov [10] from electron diffraction studies. Alapini et al. [8] have reported a high temperature phase (673–768 K), Ga_2Te_5(s), with a hexagonal structure. Tschirner et al. [19] have found Ga_2Te_5(s) by DTA. Ga_3Te_4(s), with a trigonal structure, has been reported by Lisauskas and Yasutis [20] from electron diffraction study of thin films, by Antonopoulos et al. [15] with transmission electron microscopy (TEM), and by Blachnik and Irle [9] with XRD and DTA.

The standard molar enthalpy of formation $\Delta_f H°(298\,K)$ of GaTe(s) (-125.5 ± 12.6 kJ mol^{-1}) has been selected by Mills [21] from the work of Hahn and Burow [22] by combustion calorimetry and of Abbasov et al. [16] by galvanic cell measurements. More recently, Said and Castenet [23] have reported a value of -78.8 ± 2.4 kJ mol^{-1} obtained by solution calorimetry in liquid tin and liquid gallium.

The vapor composition and the nature of the sublimation of GaTe(s) in the temperature range 903–1023 K has been reported by Plotnikov et al. [24] by mass spectrometry. They took GaTe(s) to vaporize congruently according to the reaction

$$GaTe(s) = (1/2)Ga_2Te(g) + (1/4)Te_2(g) \quad (1)$$

The temperature dependence of partial pressures p_{Ga_2Te} and p_{Te_2}, and the equilibrium constant K_p of reaction (1) in the temperture range 903–1023 K have been reported [24] as

$$\log\left(\frac{p_{Ga_2Te}}{kPa}\right) = -\left(\frac{15063 \pm 378}{T}\right) + (13.865 \pm 0.39) \quad (2)$$

$$\log\left(\frac{p_{Te_2}}{kPa}\right) = -\left(\frac{16652 \pm 759}{T}\right) + (15.115 \pm 0.88) \quad (3)$$

(Sic: Note that the unit of pressure in eqns. (2) and (3) should be pascals.)

$$\log\left(\frac{K_p}{Pa^{3/4}}\right) = -\left(\frac{11694 \pm 268}{T}\right) + (10.711 \pm 0.294) \quad (4)$$

At 1000 K, eqn. (4) yields $K_p = 0.104\ Pa^{3/4}$ for reaction (1). With Gibbs free energy functions and $\Delta H°(298\ K)$ of GaTe(s) from Mills [21], one calculates $K_p = 0.017\ Pa^{3/4}$. Substitution of the value of $\Delta H°(298\ K)$ for GaTe(s) from Said and Castanet [23] gives $K_p = 3.867\ Pa^{3/4}$. These results reveal considerable variation among reported thermodynamic properties of GaTe(s).

Second-law and third-law values of $\Delta H°(298\ K)$ (kJ mol^{-1}) of reaction (1) have been reported as 248.8 ± 9.6 and 215.3 ± 19.3 [24], respectively. With this third-law value and $\Delta_f H°(298\ K)$ (kJ mol^{-1}) of $Ga_2Te(g)$ and $Te_2(g)$ equal to 151 ± 29 [21] and 168.4 ± 0.8 [25], respectively, one obtains the $\Delta_f H°(298\ K)$ of GaTe(s) as -98 ± 24 kJ mol^{-1}. (The unit of $\Delta_f H°(298\ K)$ is sometimes expressed in kJ per one gram atom of solid or liquid, i.e. $\Delta_f H°(298\ K)$ of $Ga_{0.50}Te_{0.50}(s) = -49 \pm 12$ kJ (g atom)$^{-1}$.) The second-law value yields -131 ± 17 kJ mol^{-1}. One sees, then, a variation of some 50 kJ mol^{-1} in the reported values of $\Delta_f H°(298\ K)$ for GaTe(s).

In this paper we attempt to resolve some of the variations described above through effusion studies of GaTe(s) by the simultaneous Volmer and Knudsen method.

EXPERIMENTAL

Samples

High purity elements, 99.999% gallium (Atomergic Chemetals Corp.) and 99.9999% tellurium (Alfa Products) were used as starting materials. Three samples, labeled S1, S2, and S3, were made by heating stoichiometric quantities of the elements in evacuated sealed Vycor tubes. S1 and S2 had $X_{Te} = 0.500 \pm 0.005$ and $X_{Ga} = 0.500 \mp 0.005$; S3 had $X_{Te} = 0.440 \pm 0.005$ and $X_{Ga} = 0.560 \mp 0.005$. During preparation, all samples were heated to 1273 ± 50 K for 3–4 days and annealed at 1073 K for a week. The tubes were broken open and samples were ground and used in subsequent experiments and analyses. S1, after grinding, was transferred into another Vycor tube and the tube was sealed and reheated; the sample was then used in the same manner as S2 and S3.

Phase contents of samples and residues were analysed by Debye–Scherrer X-ray powder diffractometry (XRPD). Elemental analyses were done with a Perkin-Elmer model ICP/500 inductively coupled plasma (ICP) emission spectrometer; scandium was used as an internal reference standard [26].

Preliminary vaporization experiments

Four sets of preliminary vaporization experiments, E1, E2, E3, and E4, were done. A graphite Knudsen cell with an orifice area of $(4.88 \pm 0.74) \times 10^{-3}$ cm^2 and a transmission probability of 0.249 ± 0.004 was used in all four experiments. The Knudsen cell was radiatively heated in a resistance tube furnace in E1–E3 and was inductively heated in a radio-frequency induction furnace in E4. The setup in the induction furnace allowed one to collect effusate deposited on a glass envelope surrounding the Knudsen cell.

In E1, 253.70 mg of S2 was heated six times successively at 1073 ± 10 K. The heatings were labeled E1-1–E1-6, respectively. Subsequent to each heating, the cell was weighed, the residue was sampled for XRD analysis (except in E1-1) and the remaining residue was used in the next heating (except in E1-6). In E2, 211.10 mg of S1 was heated at 1080 ± 10 K two times successively. The heatings were labeled E2-1 and E2-2. The residues from both heatings, labeled RE2-1 and RE2-2, respectively, were sampled for XRPD and ICP analyses. In E3, 83.90 mg of S1 was heated to exhaustion at 1080 ± 10 K. In E4, 496.20 mg of S1 was heated five times successively in the temperature range 1073–1098 K. The heatings were labeled E4-1–E4-5, respectively. After each heating the cell and the residue were weighed and prepared for the next heating without removing residue. Effusates from E4-2–E4-5, labeled CE4-2–CE4-5, respectively, were collected at the end of each heating for ICP analyses. Only the final residue from E4-5, labeled RE4-5, was sampled for XRPD and ICP analyses.

Vapor pressure measurements

Vapor pressures were measured by the computer-automated simultaneous Volmer(torsion)–Knudsen(rate of mass loss) method. The apparatus and its design are described elsewhere [27–30]. Three graphite torsion cells [30], labeled TC1, TC2, and TC3 were used. TC1 had diverging right-circular-conical orifices. TC2 and TC3 had cylindrical orifices. The geometric properties of the cells are given in Table 1. The ratios of the effective orifice areas of TC1:TC2:TC3 were 7:2:1, respectively. Temperatures were measured with a Pt, Pt–10%-Rh thermocouple in a dummy cell identical in design and material to the torsion cell. The two cells were placed symmetrically, the torsion cell above and the dummy cell below the center of the furnace, and separated by 2 mm. The thermocouple was read to ± 0.1 mV (± 1 K) with a Leeds and Northrup Model 8691 potentiometer with room temperature junction. Before and after the experiments, temperatures of the dummy cell measured with the thermocouple matched within ± 5 K those measured

TABLE 1

Effusion cell parameters

Parameter [a]	TC1		TC2		TC3	
	Orifice 1	Orifice 2	Orifice 1	Orifice 2	Orifice 1	Orifice 2
θ (deg)	29.8 ± 0.5	29.3 ± 0.5	0.0 ± 0.5	0.0 ± 0.5	0.0 ± 0.5	0.0 ± 0.5
$10^3 a$ (cm^2)	6.05 ± 0.27	5.65 ± 0.26	2.98 ± 0.04	3.09 ± 0.06	2.93 ± 0.03	2.84 ± 0.04
L/r	4.62 ± 0.12	4.91 ± 0.14	3.86 ± 0.10	3.73 ± 0.10	6.82 ± 0.11	6.77 ± 0.11
d (cm)	0.800 ± 0.003	0.800 ± 0.003	0.810 ± 0.003	0.810 ± 0.003	0.792 ± 0.003	0.792 ± 0.003
f	1.093 ± 0.010	1.091 ± 0.010	0.411 ± 0.009	0.419 ± 0.010	0.287 ± 0.011	0.288 ± 0.011
W	0.907 ± 0.008	0.902 ± 0.008	0.364 ± 0.008	0.372 ± 0.008	0.252 ± 0.010	0.254 ± 0.009

[a] θ = semiapex angle; a = minimum area [28]; L/r = ratio of orifice length to minimum radius; d = moment arm; f = recoil force correction factor [28]; W = transmission probability [28].

with a calibrated optical pyrometer focused on a black body hole in the dummy cell. The accuracy of temperature measurements, then, was taken to be ±5 K, and the precision was taken to be ±1 K.

Four sets of measurements of vapor pressure vs. temperature, labeled Sets 1–4, were conducted. Sets 1 and 2 were carried out with TC1 and TC2, respectively, and Sets 3 and 4 with TC3. In Sets 1 and 2, 527.78 mg and 526.20 mg, respectively, of S2 were used. In Sets 3 and 4, 516.52 mg of S1 and 491.80 mg of S3, respectively, were used. The sample was distributed between the two chambers in the torsion cell in proportion to the effective orifice areas of the orifices [31]. A distributed temperature program [32] was chosen. At the end of each set, residues in each of the chambers were examined and analyzed by XRPD. The residues in each of the chambers from Sets 2 and 4, labeled RS2-1, RS2-2, RS4-1, and RS4-2, respectively, were analysed by the ICP method.

In Sets 1–4, three types of measurements were made simultaneously: P_V, the Volmer (or torsion) pressure [33]; P_K, the Knudsen pressure [33] calculated with the assigned molecular weight of 264 g mol^{-1} on the basis of eqn. (1); T, the temperature. The apparent molecular weight M of the effusing vapor was calculated from P_K and P_V [33]. The methods of obtaining values of these parameters have previously been described [30, 33]. Thermal functions necessary to calculate the enthalpy of the vaporization were obtained from the literature [21, 25] or estimated.

Measured vapor pressures P_m were related to vapor pressures P_0 in a hypothetical cell with orifice area of zero by [34, 35]

$$P_0 = P_m\left(1 + \frac{WA}{\alpha A_s}\right) \tag{5}$$

where α is the condensation coefficient, A is the orifice area, W is the transmission probability, and A_s is the area of the vaporizing sample.

RESULTS AND INTERPRETATION

S1, S2, and S3 had the XRPD pattern of GaTe(s) [6, 14]. Their X_{Te} from ICP analyses were 0.503 ± 0.002, 0.503 ± 0.002 and 0.436 ± 0.003, respectively.

Small residual glass particles were observed after dissolution of samples for the ICP analyses and a few milliliters of RE2-1 solution was lost during dilution to a 250 ml volumetric flask. The ICP results from all samples, residues, and effusates are shown in Table 2. Columns 1 and 2 give the analyte and its total concentration in mg l^{-1}, respectively. Columns 3 and 4 give concentrations of Ga and Te and their uncertainties in mg l^{-1} from the analyses, respectively. Uncertainties were determined from standard deviations in the slope and intercept of a calibration curve. Column 5 gives X_{Te} from the analyses and its uncertainty propagated from the uncertainties in columns 3 and 4. Column 6 gives the percentage recovery of the analyte which is a ratio of the sum of values in columns 3 and 4 and the value in column 2.

In E1, percentage mass losses from the original mass of the sample at the end of E1-1, E1-2, E1-3, E1-4, E1-5, and E1-6 were 1.5, 6.8, 43.4, 61.9, 83.2 and 97.2, respectively. The residues from E1-2, E1-3, E1-4, and E1-5 had the XRD pattern of GaTe(s) [6, 14]. The residue from E1-6 by visual inspection was metallic gallium and a black substance, but the amount was insufficient for analysis.

In E2, percentage mass losses from the original mass of the sample at

TABLE 2

ICP results[a]

Analyte	Total conc. (mg l^{-1})	Ga conc. (mg l^{-1})	Te conc. (mg l^{-1})	X_{Te}	Recovery (%)
S1	382.0	129.8 ± 0.8	240.5 ± 0.7	0.503 ± 0.002	96.9
S2	89.4	30.8 ± 0.4	57.1 ± 0.4	0.503 ± 0.002	98.4
S3	420.0	171.8 ± 1.4	243.2 ± 0.9	0.436 ± 0.003	98.8
RE2-1	97.5	37.5 ± 0.4	46.9 ± 0.4	0.406 ± 0.005	86.5
RE2-2	318.6	153.8 ± 0.7	164.8 ± 0.8	0.369 ± 0.002	97.4
RE4-5	368.0	161.6 ± 0.8	198.6 ± 1.1	0.402 ± 0.003	97.9
RS2-1	244.0	85.9 ± 0.6	145.0 ± 1.1	0.480 ± 0.004	94.6
RS2-2	319.0	110.0 ± 0.8	189.9 ± 1.4	0.485 ± 0.004	94.0
RS4-1	349.0	180.7 ± 0.8	150.7 ± 1.4	0.313 ± 0.003	95.5
RS4-2	351.0	185.1 ± 0.8	147.0 ± 0.8	0.303 ± 0.002	94.6
CE4-2	146.9	55.8 ± 0.5	86.1 ± 0.5	0.457 ± 0.004	96.6
CE4-3	128.4	41.4 ± 0.4	80.7 ± 1.1	0.561 ± 0.008	95.1
CE4-4	198.5	42.4 ± 0.4	131.6 ± 1.7	0.629 ± 0.010	87.7
CE4-5	188.0	45.1 ± 0.5	131.3 ± 0.8	0.614 ± 0.005	93.8

[a] For a description of each measured quantity, see text.

the end of E2-1 and E2-2 were 38 and 65, respectively. The residues from both heatings had the XRD pattern of GaTe(s) [6, 14], and their X_{Te} by the ICP analyses were 0.406 ± 0.005 and 0.369 ± 0.002, respectively.

In E3, percentage mass loss from the original mass of the sample was 92.9. The residue by visual inspection was a mixture of metallic gallium and a black substance.

In E4, percentage mass losses from the original mass of the sample at the end of E4-1, E4-2, E4-3, E4-4, and E4-5 were 6, 19, 31, 62, and 80, respectively. The residue from E4-5 had the XRD pattern of GaTe(s) [6, 14], and its X_{Te} by ICP analysis was 0.402 ± 0.003. The X_{Te} of the effusates collected at the end of E4-2, E4-3, E4-4, and E4-5 were found by

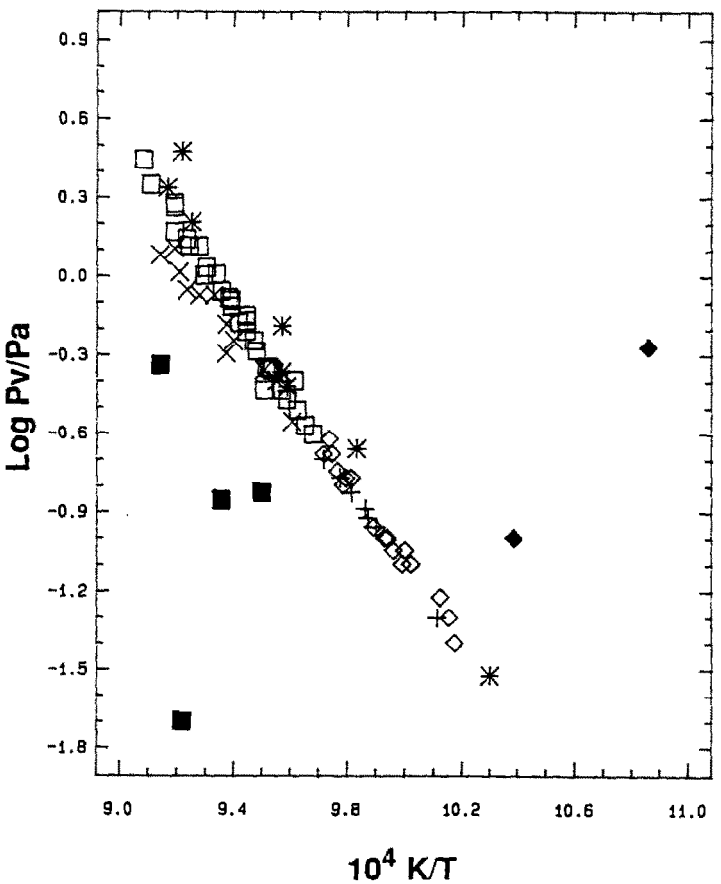

Fig. 1. Vapor pressures as functions of temperature. Initial composition of the sample GaTe, $X_{Te} = 0.503 \pm 0.002$; final composition, nearly exhaustion. Data are from Volmer measurements in Set 1: filled diamonds, Group 1; asterisks, Group 2, reactions (10) and (11); open squares, Group 3a, reactions (12) and (13); open diamonds, Group 3b, reactions (12) and (14); exes, Group 4a, reactions (15) and (16); crosses, Group 4b, reactions (12) and (14); filled squares, Group 5, reactions (17) and (18).

the ICP analyses to be 0.457 ± 0.004, 0.561 ± 0.008, 0.629 ± 0.010, and 0.614 ± 0.005, respectively.

The residue from Set 1 was similar to those from E1-6 and E3; by visual inspection it was a mixture of metallic gallium and a small amount of a black substance. In Set 3, the measurements were accidentaly terminated owing to a temperature excursion when 65% of sample mass had been effused, and no residue was available for analysis. In Sets 2 and 4, the measurements were terminated when 70% and 63%, respectively, of the original mass had effused in order to collect residues for XRPD and ICP analyses. The residues from Sets 2 and 4 had the XRD pattern of GaTe(s) [6, 14] and their X_{Te} were 0.483 ± 0.004 and 0.308 ± 0.003, respectively.

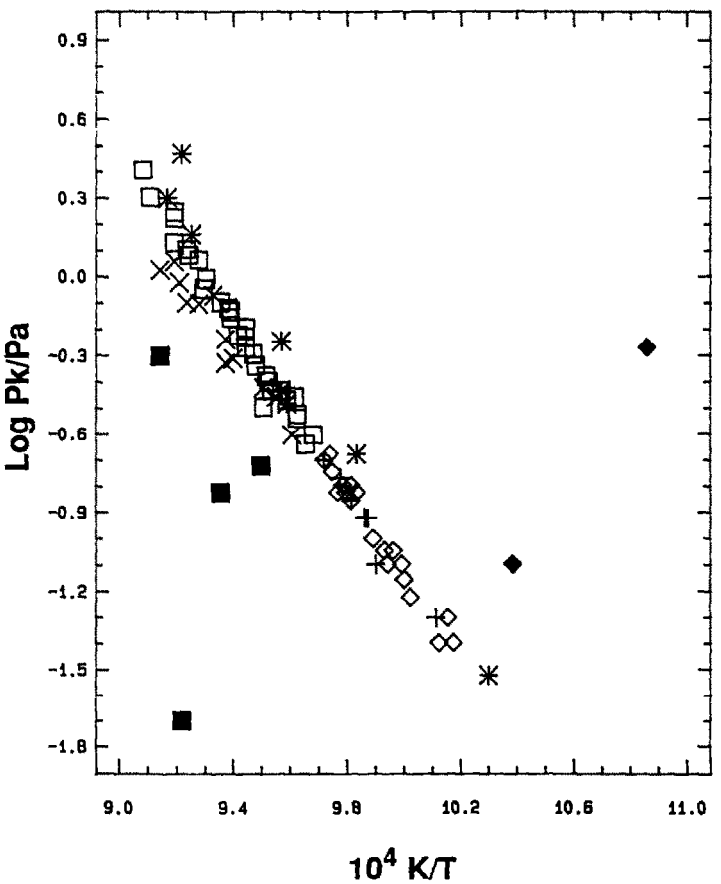

Fig. 2. Vapor pressures as functions of temperature. Initial composition of the sample GaTe, $X_{Te} = 0.503 \pm 0.002$; final composition, nearly exhaustion. Data are from Knudsen measurements in Set 1: filled diamonds, Group 1; asterisks, Group 2, reactions (10) and (11); open square, Group 3a, reactins (12) and (13); open diamonds, Group 3b, reactions (12) and (14); exes, Group 4a, reactions (15) and (16); crosses, Group 4b, reactions (12) and (14); filled squares, Group 5, reactions (17) and (18).

In Set 4, mass of the torsion cell TC3 after vapor pressure measurements was 1.7 mg lower than that obtained before the measurements.

Data from vapor pressure measurements in Set 1 are shown in Figs. 1 and 2, where the logarithms of Volmer and Knudsen pressures, respectively, are plotted vs. $1/T$. Data were divided according to their characteristics into five groups, labeled Groups 1–5. In the figures, symbols and groups relate as follows: Group 1, filled diamonds; Group 2, asterisks; Group 3, open squares and open diamonds; Group 4, exes and crosses; Group 5, filled squares. The use of two symbols in Groups 3 and 4 is for a purpose to be explained subsequently. The designs of later experiments, Sets 2–4, were influenced by an intention of testing and clarifying results from Set 1. For example: (a) in Sets 2 and 3, cells with

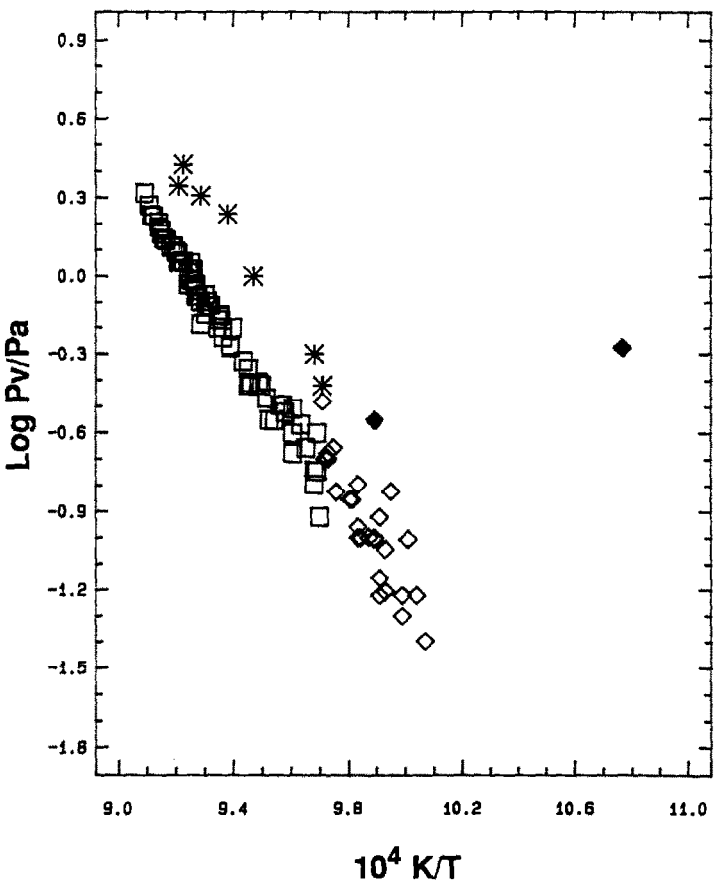

Fig. 3. Vapor pressures as functions of temperature. Initial composition of the sample GaTe, $X_{Te} = 0.503 \pm 0.002$; final composition, $X_{Te} = 0.483 \pm 0.004$. Data are from Volmer measurements in Set 2: filled diamonds, Group 1; asterisks, Group 2, reactions (10) and (11); open squares; Group 3a, reactions (12) and (13); open diamonds, Group 3b, reactions (12) and (14).

smaller orifice areas were used; (b) in Set 4, a sample with a different starting composition was used; (c) the residues from Sets 2 and 4 were chemically analyzed.

Data from Sets 2, 3, and 4 are shown in Figs. 3 and 4, Figs. 5 and 6, and Figs. 7 and 8, respectively. There are three groups (1, 2, and 3) in Sets 2 and 3 and two groups (1 and 3) in Set 4. Assignment of the groups and the symbols for them were made on the basis of results from Set 1. The groups are identified by the properties, i.e. the range of the percentages of sample mass effused from the cell and the average value of the apparent molecular weight, which are given in Table 3. Columns 1 and 2 give the group and the property, respectively. Columns 3–6 give the value of the property of each group in each set.

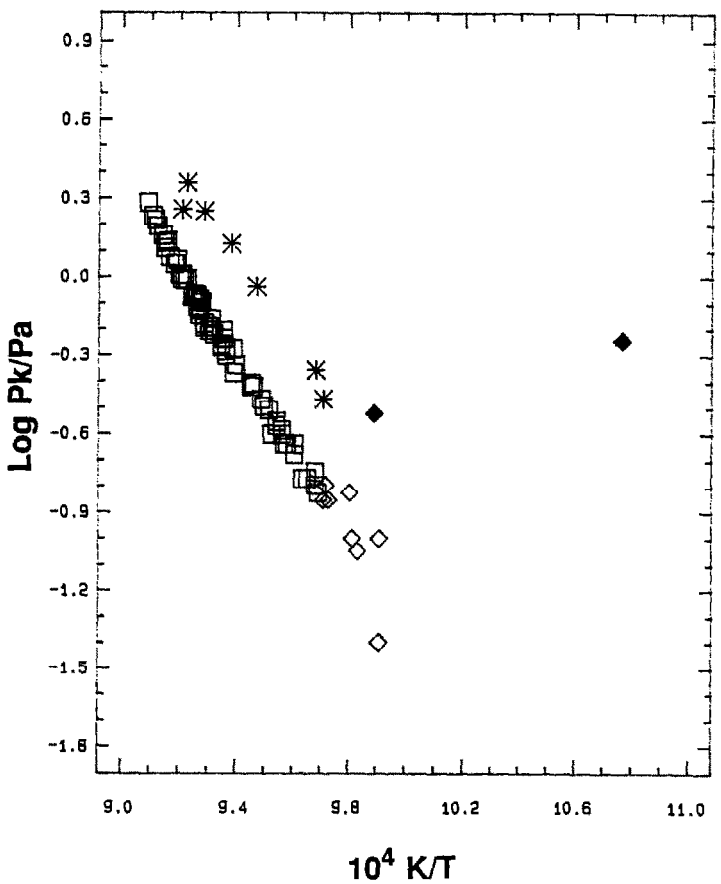

Fig. 4. Vapor pressures as functions of temperature. Initial composition of the sample GaTe, $X_{Te} = 0.503 \pm 0.002$; final composition, $X_{Te} = 0.483 \pm 0.004$. Data are from Knudsen measurements in Set 2: filled diamonds, Group 1; asterisks, Group 2, reactions (10) and (11); open squares, Group 3a, reactions (12) and (13); open diamonds, Group 3b, reactions (12) and (14).

The average values of the apparent molecular weights (M) from all data in each of Sets 1, 3, and 4 (222 ± 39, 237 ± 42, and 232 ± 35 g mol^{-1} respectively) were 7–17% too low relative to the molecular weight of Te_2 (255) or Ga_2Te (267), i.e. P_K was approximately 4–9% lower than P_V. The average value of M from all data in Set 2 (200 ± 38 g mol^{-1}) was 24% lower than 267, i.e. P_K was 13% lower than P_V. The average value of all data in all sets was 219 ± 38 g mol^{-1}.

Data in sets 1–4 are shown in Tables B1–B4 in Appendix B. In each table, column 1 gives the order in which data were obtained, columns 2–6 give the assigned group, the temperature, the Volmer pressure, the Knudsen pressure, the apparent molecular weight, and the percentage mass loss at the end of the measurement, respectively.

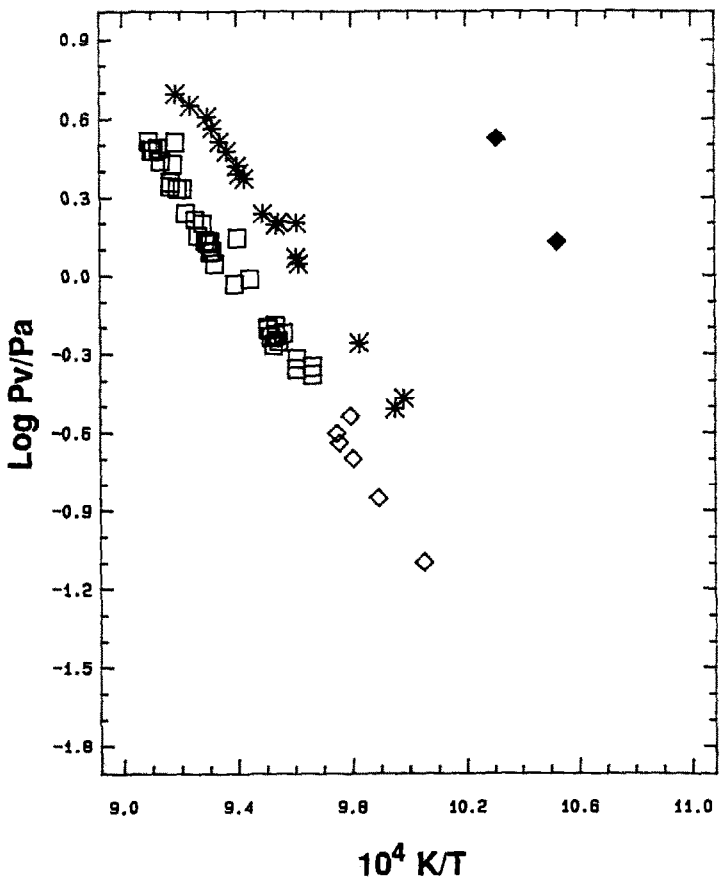

Fig. 5. Vapor pressures as functions of temperature. Initial composition of the sample GaTe, $X_{Te} = 0.503 \pm 0.002$; final composition, unavailable. Data are from Volmer measurements in Set 3: filled diamonds, Group 1; asterisks, Group 2, reactions (10) and (11); open squares, Group 3a, reactions (12) and (13); open diamonds, Group 3b, reactions (12) and (14).

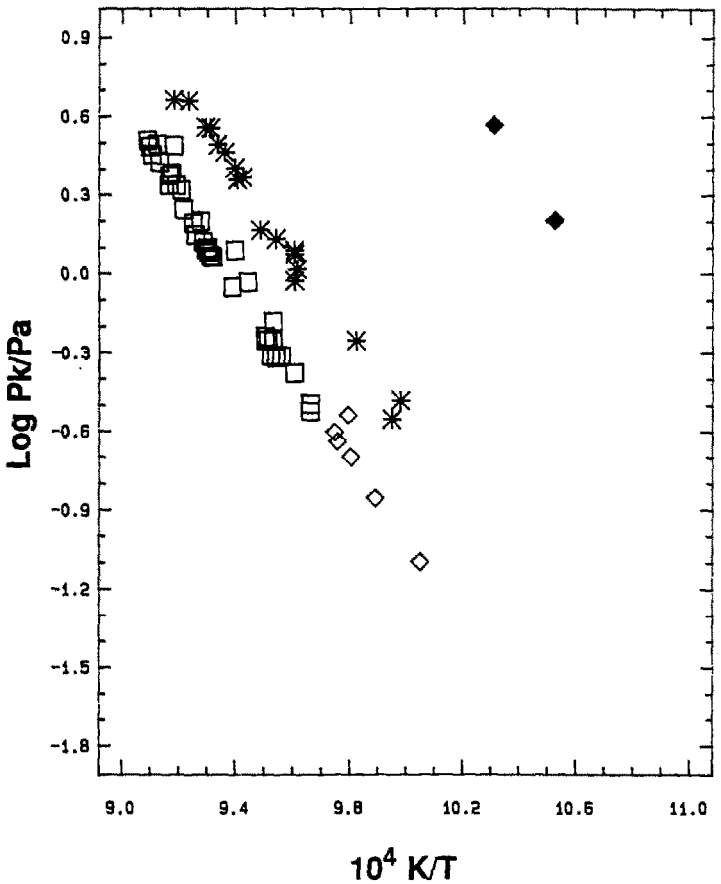

Fig. 6. Vapor pressures as functions of temperature. Initial composition of the sample GaTe, $X_{Te} = 0.503 \pm 0.002$; final composition, unavailable. Data are from Knudsen measurements in Set 3: filled diamonds, Group 1; asterisks, Group 2, reactions (10) and (11); open squares, Group 3a, reactions (12) and (13); open diamonds, Group 3b, reactions (12) and (14).

Interpretation of the present results called for modification of the reported phase diagram [5–9, 23] of the Ga–Te system for our pressure range, where equilibrium vapor was always present. The phase Ga_3Te_2(s) at $X_{Te} = 0.40$ reported by Newman et al. [6] was not observed; a Ga-rich phase (β) at $X_{Te} = 0.49$ was discovered. Two quadruple points (temperatures and pressures at which three condensed phases and vapor are in equilibrium) were seen, one at 1029 ± 12 K and 0.22 (+0.10/−0.09) Pa and the other at 968 ± 42 K and 0.026 (+0.094/−0.022) Pa.

The temperature–composition diagram modified to conform to our results is presented in Fig. 9. The main features of the diagram remain the same as those in the published phase diagrams [5–9, 23] (without a Ga_3Te_2(s) [6] phase) and are drawn in thick lines. The phase β is

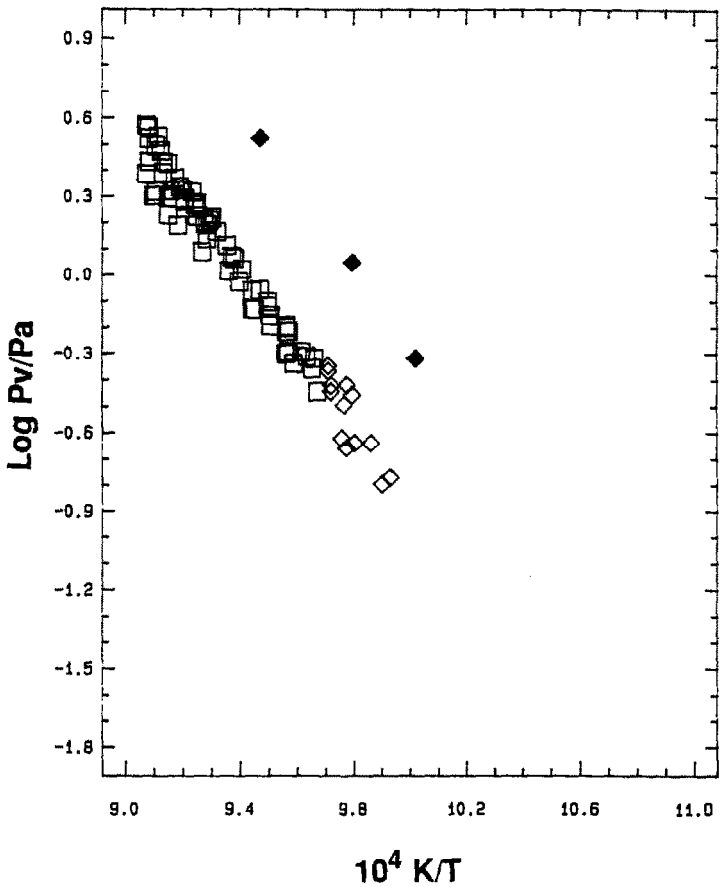

Fig. 7. Vapor pressures as functions of temperature. Initial composition of the sample $X_{Te} = 0.436 \pm 0.003$; final composition, $X_{Te} = 0.308 \pm 0.003$. Data are from Volmer measurements in Set 4: filled diamonds, Group 1; open squares, Group 3a, reactions (12) and (13); open diamonds, Group 3b, reactions (12) and (14).

represented by a vertical thin line at $X_{Te} = 0.49$. In this work, β was observed in the temperature range 970–1089 K and the pressure range 0.03–5 Pa.

To comply with the phase diagram in Fig. 9 we divided data of Groups 3 and 4 into two subgroups: those above the quadruple point (1029 ± 12 K) were labeled 3a and 4a; those below 1029 ± 12 K were labeled 3b and 4b. Subgroups 3a and 3b were represented by open squares and open diamonds, respectively in Figs. 1–8. Subgroups 4a and 4b which obtained only in Set 1, were represented by crosses and exes, respectively in Figs. 1 and 2. Without a $Ga_3Te_2(s)$ phase, data in Group 3b should be indistinguishable from those in Group 4b.

The pressure–composition phase diagrams in two temperature ranges, (above and below 1029 ± 12 K) are shown in Figs. 10 and 11, respectively.

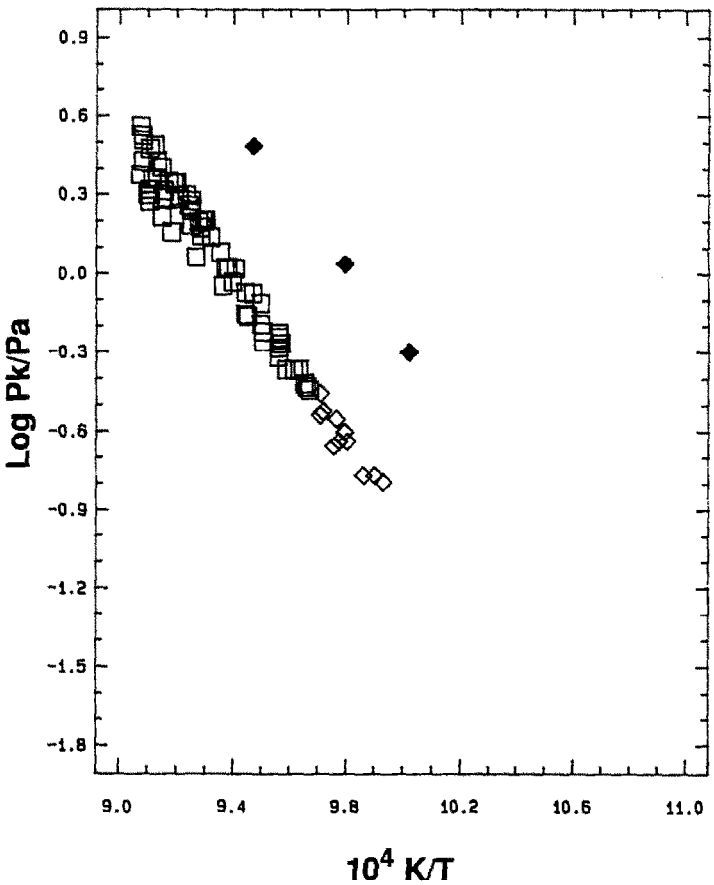

Fig. 8. Vapor pressures as functions of temperature. Initial composition of the sample $X_{Te} = 0.436 \pm 0.003$; final composition, $X_{Te} = 0.308 \pm 0.003$. Data are from Knudsen measurements in Set 4: filled diamonds, Group 1; open squares, Group 3a, reactions (12) and (13); open diamonds, Group 3b, reactions (12) and (14).

In Figs. 10 and 11, a vertical line represents a condensed phase with a practically unique composition, i.e. GaTe and β. A shaded area confined by curved lines represents a solid or liquid solution with a range of composition, i.e. L1 and L2. The curved line bounding open areas on the right and below represents the composition of vapor in equilibrium with the condensed phase. The horizontal lines x, y, y′, and z represent the pressures at which two condensed phases are in equilibrium with vapor.

In Group 1 of each set, the vapor pressures were bivariant, i.e. the vapor pressure at a given temperature decreased with time during the short time of each measurement. Group 1 persisted until the sample lost 1–3% of its initial mass. In Group 1, the sample probably outgassed or lost excess tellurium as $Te_2(g)$. Data in Group 1 are shown in Tables B1–B4 and Figs. 1–8 but are not included in the subsequent analysis. The

TABLE 3

Properties of the group: percent mass loss; average apparent molecular weight; number of data of each group in each set

Group	Property	Set 1	Set 2	Set 3	Set 4
1	% Mass loss	0–3 ± 1	0–2 ± 1	0–3 ± 1	0–2 ± 1
	Ave. M	217 ± 67	305	350 ± 37	252 ± 33
	No. of data	2	1	2	3
2	% Mass loss	3–10 ± 2	2–10 ± 2	3–23 ± 2	–
	Ave. M	225 ± 27	196 ± 22	230 ± 36	–
	No. of data	8	7	18	–
3	% Mass loss	10–80 ± 2	10–70 ± 2	23–65 ± 2	2–65 ± 5
	Ave. M	217 ± 29	199 ± 38	235 ± 37	232 ± 35
	No. of data	49	71	42	71
3a	Ave. M	219 ± 20	200 ± 35	237 ± 36	237 ± 27
	No. of data	31	65	37	60
3b	Ave. M	231 ± 41	189 ± 64	220 ± 46	201 ± 55
	No. of data	18	6	5	11
4	% Mass loss	80–96 ± 1	–	–	–
	Ave. M	213 ± 24	–	–	–
	No. of data	18	–	–	–
4a	Ave. M	212 ± 13	–	–	–
	No. of data	12	–	–	–
4b	Ave. M	216 ± 41	–	–	–
	No. of data	6	–	–	–
5	% Mass loss	96–98 ± 1	–	–	–
	Ave. M	326 ± 69	–	–	–
	No. of data	4	–	–	–
All	Ave. M	222 ± 39	200 ± 38	237 ± 42	232 ± 35
	No. of data	81	79	62	74

vapor pressures in Group 2 were univariant, i.e. the vapor pressure at a given temperature was constant with time. Group 2 persisted until the sample lost 10–20% of its initial mass. The univariance of vapor pressure implied the presence of two condensed phases in equilibrium with the vapor, as shown by the horizontal line x in Figs. 10 and 11. GaTe(s) was in equilibrium with β and vapor. The value of X_{Te} of β is taken to be between 0.503 ± 0.002 and 0.483 ± 0.004, i.e. the compositions of the starting material and the residue from Set 2, respectively. The value 0.490 ± 0.005 and the formula $GaTe_{0.96\pm0.02}$(s) were assigned.

The vapor pressures in Subgroups 3a and 3b were univariant until the sample lost 70–80% of its initial mass; a slight curvature in the $\log P$ vs. $1/T$ plot of Subgroup 3a above the quadruple point (1029 ± 12 K) indicated a temperature dependence of the composition of the condensed

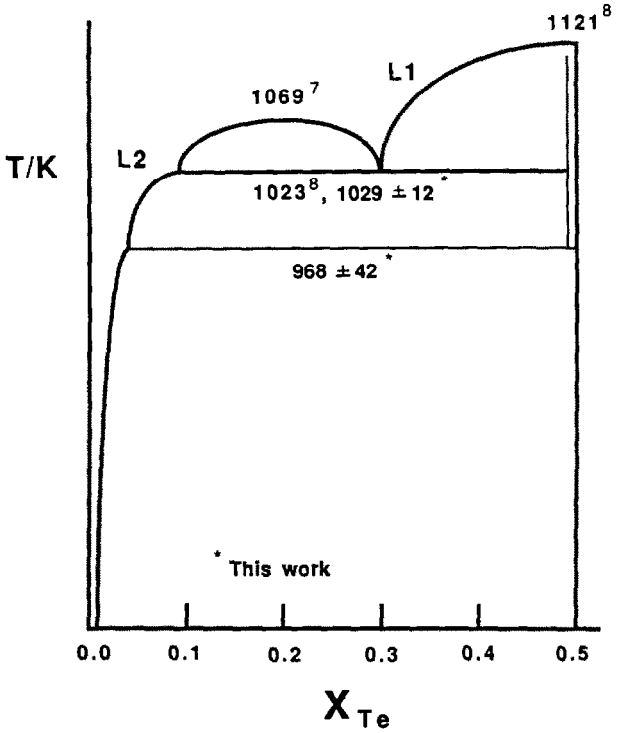

Fig. 9. Temperature–composition phase diagram of GaTe–Ga system by Wobst [7], Alapini et al. [8], and Blanchnik and Irle [9]. Thin lines are from this work and apply at the low pressures in the effusion cell.

phase. Above 1029 ± 12 K, β was in equilibrium with vapor and L1, whose composition depended measurably on temperature; below 1029 ± 12 K, β was in equilibrium with vapor and L2, whose composition variation with temperature was not observed. Only at 1029 ± 12 K are the four phases β, L1, L2, and vapor in equilibrium. The univariant vapor pressures in Subgroups 3a and 3b were represented by horizontal lines y in Fig. 10 and y' in Fig. 11, respectively.

In Subgroup 4a, the vapor pressures were initially bivariant (i.e. the vapor pressure at a given temperature decreased with time) then they became univariant and those in Subgroup 4b were univariant. Group 4 persisted until the sample lost 90–96% of its initial mass. During collection of data in Subgroup 4a, phases L1, L2, and vapor were present. The univariance in Group 4a was represented by the horizontal line z in Fig. 10. Temperature dependence of the composition of the liquids was not revealed because few data were collected in this subgroup.

Vapor pressures in Subgroups 3b and 4b as shown in Figs. 1 and 2 were indistinguishable. This fact indicates that the chemical reactions occurring while collecting data of Subgroups 3b and 4b were the same. On this

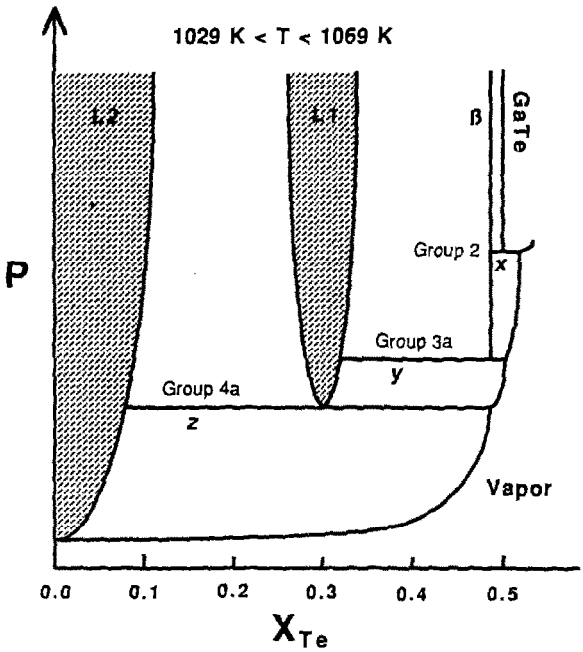

Fig. 10. Proposed pressure–composition phase diagram of the GaTe—Ga system at intermediate temperatures (1029 K < T < 1069 K).

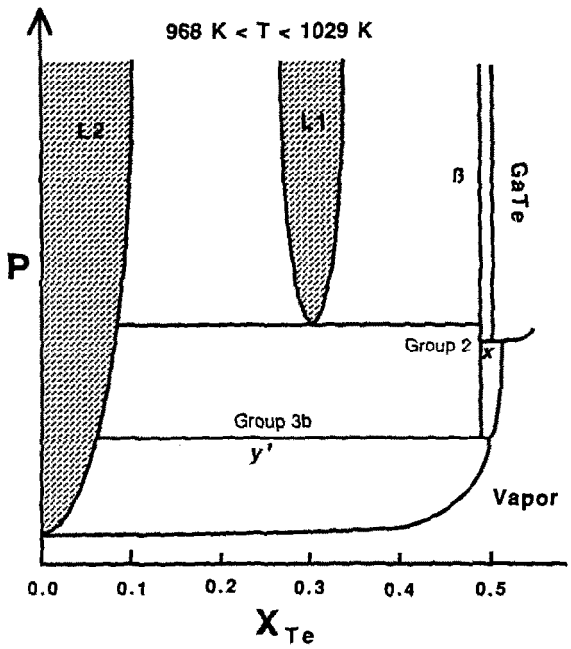

Fig. 11. Proposed pressure–composition phase diagram of the GaTe—Ga system at low temperatures (968 K < T < 1029 K).

basis, the presence of Ga_3Te_2(s) (reported by Newman et al. [6]) was ruled out in this work.

The vapor pressures in Group 5 were bivariant until the end of the measurement. In this group, L2 vaporized as its composition approached that of liquid gallium.

A schematic pressure–temperature phase diagram projected along the composition axis is given in Fig. 12. Lines AE, BD, CD, and DE were fitted to Groups 2, 3a, 4a, and 3b, respectively, of Volmer data in Set 1. Line EF is drawn and placed between the extensions of AE and DE. No data were obtained below the temperature and pressure at point E. Each area in the phase diagram represents a projection along the composition axis of a T–P–X volume within which specific phases are stable. Within the area above line AEF, GaTe(s) is stable. Within the area between lines AE and BDE, β and vapor are stable. Within the area between lines BD and CD, L1 and vapor are stable. Within the area below line CDEF, L2

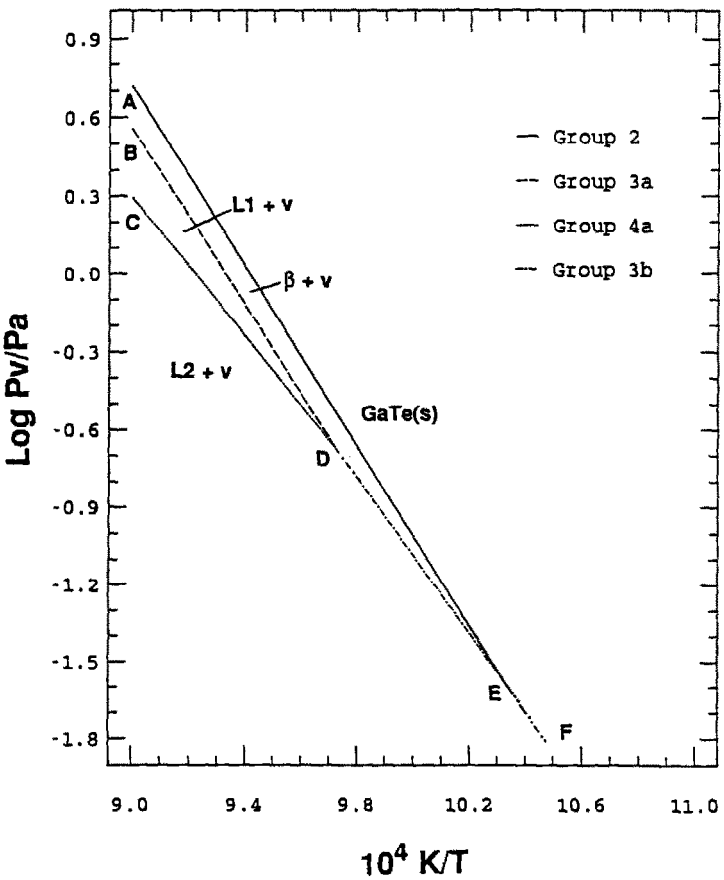

Fig. 12. Projection along a composition axis of the pressure–temperature phase diagram of the GaTe–Ga system; data from Set 1, Volmer pressures.

and vapor are stable. Below 0.22 (+0.10/−0.09) Pa, L1 is unstable; below 0.026 (+0.094/−0.022) Pa, β is unstable. The two quadruple points at D and E are estimated from the intersections of lines BD and CD and AE and DE, respectively. At D, β, L1, L2, and vapor are at equilibrium. At E, GaTe(s), β, L2, and vapor are at equilibrium.

Vaporization equations were produced, in line with the following five principles.

(1) Mass spectrometry [24] has shown that samples in the composition range $X_{Te} = 0.30$–0.50 effuse to give but two important gaseous species, $Ga_2Te(g)$ and $Te_2(g)$.

(2) Stoichiometric considerations require that in the composition range $X_{Te} = 0$–0.30, composition of the vapor be more gallium-rich than Ga_2Te. To meet this requirement with known species we took the vapor to be composed of $Ga_2Te(g)$ and Ga(g).

(3) Representation of an incongruent vaporization reaction requires a minimum of two simultaneous chemical equations.

(4) An incongruent vaporization in a two-component system with two vapor species A(g) and B(g) can be represented by any two of the four equations

$$AB_x(s) = AB_y(s) + (x - y)B(g) \quad (6)$$

$$AB_y(s) = (y/x)AB_x(s) + (1 - y/x)A(g) \quad (7)$$

$$AB_x(s) = A(g) + xB(g) \quad (8)$$

$$AB_y(s) = A(g) + yB(g) \quad (9)$$

The appropriate choice of two would be influenced by the nature of the system to be represented.

(5) Each equation was balanced such that one mole of gas was produced.

Vapor pressures in Group 2 were produced by the simultaneous but nonequivalent reactions (10) and (11), with reaction (10) predominating.

$$50GaTe(s) = 50GaTe_{0.96\pm0.02}(s) + Te_2(g) \quad (10)$$

$$25GaTe_{0.96\pm0.02}(s) = 23GaTe(s) + Ga_2Te(g) \quad (11)$$

Vapor pressures in Subgroup 3a were produced by the simultaneous but nonequivalent reactions (12) and (13), with reaction (12) predominating.

$$1.370GaTe_{0.96\pm0.02}(s) = 0.685Ga_2Te(g) + 0.315Te_2(g) \quad (12)$$

$$3.763GaTe_{0.96\pm0.02}(s) = 0.538L1\ (X_{Te} = 0.30 \pm 0.03, \text{“}Ga_7Te_3\text{”}) + Te_2(g) \quad (13)$$

Vapor pressures in Subgroup 3b were produced by the simultaneous but nonequivalent reactions (12) and (14), with reaction (12) predominating.

$$2.356GaTe_{0.96\pm0.02}(s) = 0.262L2\ (X_{Te} = 0.10 \pm 0.03, \text{“}Ga_9Te\text{”}) + Te_2(g) \quad (14)$$

Choice of eqns. (12)–(14) from general equations (6)–(9) was made to give positive balancing numbers.

Vapor pressures in Subgroup 4a were produced by the simultaneous but nonequivalent reactions (15) and (16), with reaction (15) predominating.

$$0.25L1\ (X_{Te} = 0.30 \pm 0.03, \text{“}Ga_7Te_3\text{”}) = 0.75Ga_2Te(g) + 0.25Ga(g) \quad (15)$$

$$0.125L2\ (X_{Te} = 0.10 \pm 0.03, \text{“}Ga_9Te\text{”}) = 0.125Ga_2Te(g) + 0.875Ga(g) \quad (16)$$

Compositions of L1 and L2 are temperature dependent. The compositions arbitrarily assigned to them in eqns. (13)–(16) were estimated from those at the monotectic temperature in the published phase diagram [5–9, 23].

Vapor pressures in Group 5 were produced by the simultaneous but nonequivalent reactions (17) and (18), with reaction (17) predominating.

$$Ga_2Te(ls) = Ga_2Te(g) \quad (17)$$

$$Ga(ls) = Ga(g) \quad (18)$$

in which ls denotes the liquid solution.

To determine thermodynamic functions of the reactions above, it was necessary to determine the vapor compositions. An equation for vapor composition is derived in Appendix A1. The result is eqn. (A15). To use eqn. (A15), the starting and final compositions of the condensed phase $X^s_A(0)$ and $X^s_A(\tau)$, respectively, and the fraction of the sample mass effused at a constant temperature $f(\tau)$, must be known. The values of these parameters were obtained from ICP results on starting materials and residues given in Table 2 and from mass loss data given in Table 3. The subsequent equation, (eqn. (A16)), specifies an alternative expression for the sample composition in terms of Te_2 as a component instead of Te.

In Group 2, the initial X_{Te} of the condensed phase was 0.503 ± 0.002 and the final X_{Te} after the sample lost 10–20% of its mass was 0.490 ± 0.005. With eqns. (A15) and (A16), X_{Te_2} of the vapor was calculated to be in the range 0.49–0.40; the value 0.45 ± 0.04 was selected. The equilibrium constants K_p of reactions (10) and (11) were

$$K_p(10) = P_{Te_2} = X_{Te_2}P = (0.45 \pm 0.04)P \quad (19)$$

$$K_p(11) = P_{Ga_2Te} = X_{Ga_2Te}P = (0.55 \mp 0.04)P \quad (20)$$

where P is the total pressure.

In Group 3, the initial X_{Te} of the condensed phase was 0.490 ± 0.005 and the final X_{Te} after the sample lost 70% of its mass was 0.483 ± 0.004. With eqns. (A15) and (A16), X_{Te_2} of the vapor was calculated to be 0.33 ± 0.04 and K_p of reactions (12) and (13) were

$$K_p(12) = P_{Ga_2Te}^{0.685} P_{Te_2}^{0.315} = (0.54 \mp 0.04)P \quad (21)$$

$$K_p(13) = P_{Te_2} = X_{Te_2}P = (0.33 \pm 0.04)P \quad (22)$$

K_p of reaction (14) is the same as that of reaction (13).

Owing to the lack of information on compositions of the vapor phase in the range $0.30 > X_{Te} > 0.10$, the K_p values and consequently the standard molar heats of reactions (15)–(17) were not determined.

Existing literature values [21, 36] of Giauque functions of selenides and tellurides of gallium and indium were used to test applicability of Kopp's rule [37] in these systems, i.e. additivity of heat capacities would lead directly to additivity of Giauque functions. The ratio of $\phi°(1000\,K)$ of $In_2Se_3(s)$ to that of InSe(s) is 2.43. The same ratio for $Ga_2Se_3(s)$ and GaSe(s) is 2.52. With this justification, $\phi°$ in the Ga–Te system was taken to be directly proportional to the number of gram atoms involved in order to calculate $\phi°$ of $GaTe_{0.96\pm0.02}(s)$ from that of GaTe(s). Those of L1 and L2 were calculated [21] from the enthalpy functions, $H° - H°(298\,K)$, and the standard entropy, $S°(1114\,K)$ [38], of the liquids. The enthalpy functions were calculated with the assumption that the standard heat capacity $C_p°$ of the liquids [39] was constant in the temperature range 298–1103 K. The same procedure, applied to high temperature liquids with known enthalpy functions [40] gave values a few percent too high. Consequently, the enthalpy functions obtained by this procedure for L1 and L2 were reduced by 5%. Giauque functions used in this work are given in Table 4.

With eqn. (5), plots of Volmer and Knudsen pressures as a function of orifice area at 1050 K from Group 2 of Sets 1–3 and Group 3 of Sets 1–4 are shown in Figs. 13 and 14, respectively. The abcissa is $1/P$ and the

TABLE 4

Standard Giauque functions $\phi°(T)$ ($J\,mol^{-1}\,K^{-1}$) [a]

T (K)	GaTe(s)	$GaTe_{0.96}(s)$	L1	L2	$Ga_2Te(g)$	$Te_2(g)$
900	107.9	105.9	614.2	698.4	352.1	284.3
1000	111.8	109.7	643.5	721.6	356.3	287.0
1100	115.6	113.4	671.2	743.4	360.2	289.5

[a] $\phi°(T) = -[G°(T) - H°(298\,K)]/T$.

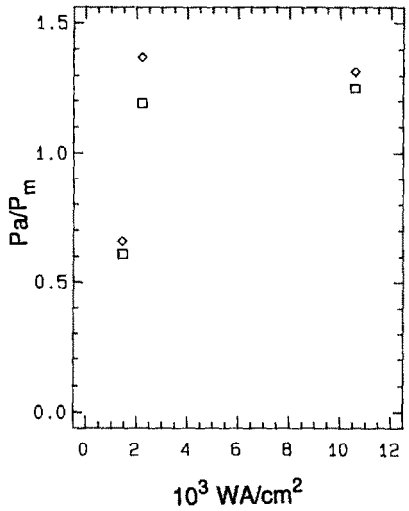

Fig. 13. Plot of $1/P_m$ vs. WA at 1050 K. Data from Group 2 of Sets 1, 2, and 3: squares, Volmer data; diamonds, Knudsen data. $WA_{Set\,3}:WA_{Set\,2}:WA_{Set\,1} = 1:2:7$.

ordinate is the effective orifice area, WA. Volmer and Knudsen data are represented by squares and diamonds, respectively. The closed symbols in Fig. 14 are the data from Set 4.

The temperature dependences of the measured vapor pressures in Group 2 of Set 3 are given by

$$\log P_V = -15842 \pm 415\left(\frac{1}{T} - 9.529 \times 10^{-4}\right) + 0.210 \pm 0.009 \qquad (23)$$

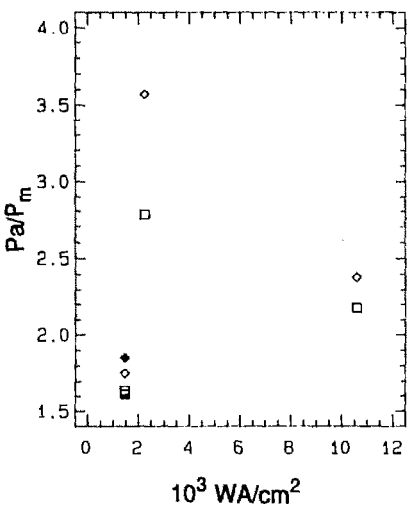

Fig. 14. Plot of $1/P_m$ vs. WA at 1050 K. Data from Group 3a of Sets 1, 2, 3, and 4: squares, Volmer data; diamonds, Knudsen data; closed symbols, from Set 4. $WA_{Set\,3}:WA_{Set\,2}:WA_{Set\,3} = 1:2:7$ and $WA_{Set\,3} = WA_{Set\,4}$.

$$\log P_K = -16073 \pm 482\left(\frac{1}{T} - 9.529 \times 10^{-4}\right) + 0.178 \pm 0.010 \quad (24)$$

and those in Group 3b of Set 3 are given by

$$\log P_V = -18292 \pm 3120\left(\frac{1}{T} - 9.965 \times 10^{-4}\right) - 0.879 \pm 0.049 \quad (25)$$

$$\log P_K = -16072 \pm 426\left(\frac{1}{T} - 9.850 \times 10^{-4}\right) - 0.778 \pm 0.005 \quad (26)$$

where log means $\log_{10}$.

The standard molar enthalpy of reactions (10)–(14) calculated from the measured pressures in Sets 3 and 4 are given in Table 5. Columns 1 and 2 give the reaction and the type of measurement, respectively. Columns 3–6 give the second and the third law values from Sets 3 and 4, respectively. Column 7 gives the selected value which is the mean of those in columns 5 and 6.

From reactions (10) and (11), $\Delta H°(298\,K)$ of reaction (1), (221.2 ± 0.2 kJ) was obtained. From this and $\Delta_f H°(298\,K)$ of $Ga_2Te(g)$ [21] and $Te_2(g)$ [25] (−151 ± 29 and 168.4 ± 0.8 kJ mol^{-1}, respectively) one finds $\Delta_f H°(298\,K)$ of $Ga_{0.50}Te_{0.50}(s)$, $Ga_{0.51}Te_{0.49}(s)$, L1 ($Ga_{0.70}Te_{0.30}$), and L2 ($Ga_{0.90}Te_{0.10}$) to be −52.0 ± 7.5, −51.5 ± 7.5, −37 ± 10, and −25 ± 13 kJ (g atom)$^{-1}$, respectively.

TABLE 5

Standard molar enthalpy of reactions (10)–(14)

Reaction No.	Type	$\Delta H°(298\,K)$ (kJ mol^{-1})				
		Second law		Third law		Sel. value
		Set 3	Set 4	Set 3	Set 4	
10	V	325 ± 8	–	293.0 ± 0.2	–	293.4 ± 0.2
	K	329 ± 9	–	293.7 ± 0.2	–	
11	V	312 ± 8	–	295.3 ± 0.2	–	295.7 ± 0.2
	K	316 ± 9	–	296.0 ± 0.2	–	
12	V	365 ± 60	354 ± 59	303.0 ± 0.9	301.6 ± 0.4	303 ± 1
	K	323 ± 8	278 ± 30	304.5 ± 0.1	303.2 ± 0.2	
13	V	271 ± 9	236 ± 8	349.2 ± 0.3	349.5 ± 0.3	349.6 ± 0.6
	K	296 ± 8	250 ± 9	349.8 ± 0.2	350.0 ± 0.3	
14	V	354 ± 60	343 ± 59	340.6 ± 0.9	340.1 ± 0.4	341 ± 1
	K	213 ± 8	267 ± 30	342.6 ± 0.2	341.8 ± 0.3	

DISCUSSION

The vapor pressures over the GaTe–Ga system were measured in the temperature range 921–1102 K. GaTe(s) was found to vaporize incongruently by reactions (10) and (11), but the composition of the vapor was nearly equal to that of the solid. The result was that a large portion of sample vaporized while only a small change occurred in the composition of the condensed phase. Throughout all effusion experiments, samples became progressively gallium-rich. Ultimately a small amount of metallic gallium was found as a residue. The appearance of metallic gallium was probably due to near exhaustion of tellurium from L2 and then freezing out of the Te-containing phase when the sample cooled to room temperature; the small amount of black substance would be the precipitate.

Some possibility remains that GaTe(s) vaporizes congruently in a temperature range outside 921–1102 K for which this work was done. Moreover, the present results do not entirely eliminate the possibility of congruent vaporization in the lower part of the present range. Isothermal effusion experiments were done only in 1080 ± 10 K. No doubt exists that GaTe(s) effuses incongruently at and above that temperature.

Vapor pressures from Set 2 were unusually low in both Volmer and Knudsen pressures as shown in Figs. 13 and 14, and thus eqn. (5) was not used to obtain the vapor pressure at orifice area of zero. The variation from eqn. (5) is well outside the precision of our method. An explanation of the dependence of vapor pressures on orifice area in this system will involve chemical kinetic factors which complicate the effusion process beyond the simple model which underlies eqn. (5). The vapor pressures and thermodynamic properties reported in this work were then chosen from Sets 3 and 4 in which the cell with the smallest orifice area was used.

With Volmer–Knudsen measurements [27–30], it is not possible to distinguish the gaseous species Ga_2Te and Te_2 because their molecular weights of 267 and 255, respectively, are practically the same. However, the apparent molecular weights averaged from data in Groups 2–4 of every set (219 ± 38) were lower than that of either species. Such a result might imply that the vapor contained some molecules lighter than the two species considered, e.g. GaTe(g), Te(g), or Ga(g). The vapor pressure of Ga(l) is too low to provide any important amount of Ga(g), except in Group 5. The equilibrium constant of dissociation of Te_2(g) forbids significant partial pressure of Te(g) under the conditions of this study. To account for the molecular weight observed, the vapor would have to contain more than 50% GaTe(g), and that, in turn, implies a $\Delta_f H°(298\ \mathrm{K})$ for GaTe(g) of less than 178 kJ mol^{-1}. The $\Delta_f H°(298\ \mathrm{K})$ of GaTe(g) calculated from the gaseous equilibrium between GaTe(g), Ga_2Te(g), and Te_2(g) [41] is 197 ± 18 kJ mol^{-1}. This result, combined with results from

mass spectrometry which reveal GaTe(g) to be minor, eliminates that species as being important. Reaction with the graphite crucible to make CTe(g) did not occur. Mass loss from the crucible during experiments was always less than 1.7 mg and some of that resulted from physical loss during removing of residues. The entire 1.7 mg of graphite could not make enough CTe(g) to account for the effect. Moreover, no CTe^+ was reported in the mass spectrometric study with a graphite crucible. We believe the explanation of the low molecular weights and the effect of orifice area on vapor pressure observed in this study must lie in a better understanding of effusion kinetics in the Ga—Te system.

The XRPD phase analysis of samples S1, S2, S3, and the residues at room temperature showed only the pattern of GaTe(s). The amorphous character of metallic gallium prevented its observation. Failure to completely recover the specimens in the ICP analysis, as shown in the last column of Table 2, resulted because samples and residues contained glass particles or possibly crucible material. The 86.5% recovery in RE2-1 was due to the reported error in transferring solution. In the case of condensed effusates, the incomplete recovery was surely due to incomplete collection of effusates on the glass envelope.

The $\Delta H°(298\,K)$ values of reactions (10)–(14) presented in Table 5 were taken as averages of the third-law values from Sets 3 and 4. Uncertainties given for these values are the standard deviations from statistical analyses. Values by the second-law method were significantly different and were not used. The preference for the third-law over the second-law values has been discussed elsewhere [29, 33].

For the $\Delta H_f°(298\,K)$ of GaTe(s) and $GaTe_{0.96\pm0.02}$(s), we recommend the values -104 ± 15 and -101 ± 15 kJ mol^{-1}, respectively.

REFERENCES

1 N.A. Gasanova and G.A. Akhundov, Opt. Spectrosk, 18 (1965) 413.
2 F. Consadori and J.L. Brebner, Solid State Commun., 12 (1973) 179.
3 G. Levêque, C.G. Olson and D.W. Lynch, J. Phys. (Paris), 45 (1984) 1699.
4 Mitsubishi Electric Corp. Jpn. Kokai Tokkyo Koho, JP 60,115,034 [85,115,034] (Cl G11B7/24), 21 June 1985, Appl. 83/222,334. 25 November 1983.
5 W. Klemm and H.U.V. Vogel, Z. Anorg. Chem., 219 (1934) 45.
6 P.C. Newman, J.C. Brice and H.C. Wright, Philips Res. Rep., 16 (1961) 41.
7 M. Wobst, Scripta Metall., 5 (1971) 583.
8 F. Alapini, J. Flahaut, M. Guittard, A. Jaulmes and M. Julien-Pouzol, J. Solid State Chem., 28 (1979) 309.
9 R. Blachnik and E. Irle, J. Less-Common Met., 113 (1985) L1.
10 S.A. Semiletov and V.A. Vlasov, Sov. Phys. Crystallogr., 8 (1964) 704.
11 H. Hahn, Angew. Chem., 65 (1953) 538.
12 K. Schubert, E. Dorre and E. Cunzel, Naturwissenschaften, 41 (1954) 448.
13 M. Julien-Pouzol, S. Jaulmes, M. Guittard and F. Alapini, Acta Crystallogr., Sect. B, 35 (1979) 2848.

14 Th. Karakostas, J.G. Antonopoulos, S. Kokkou, G.L. Bleris and N.A. Economou, Phys. Status Solidi A, 59 (1980) K17.
15 J.G. Antonopoulos, Th. Karakostas, G.L. Bleris and N.A. Economou, J. Mater. Sci., 16 (1981) 733.
16 A.A. Abbasov, A.V. Nikolskaya, Y.I. Gerasimov and V.P. Vasilev, Dokl. Phys. Chem., 156 (1964) 596.
17 J.W. Wooley and B.R. Pamplin, J. Electrochem. Soc., 108 (1961) 874.
18 P.C. Newman and J.A. Cundall, Nature, 200 (1963) 876.
19 H.-U. Tschirner, B. Garlipp, and R. Rentzsch, Z. Metallkd., 77 (1986) 811.
20 V.S. Lisauskas and V.V. Yasutis, Litov. Fiz. Sb. SSSR, 12 (1963) 877.
21 K.C. Mills, Thermodynamic Data for Inorganic Sulphides, Selenides and Tellurides, Butterworths, London, 1974.
22 H. Hahn and F. Burrow, Angew. Chem., 68 (1956) 382.
23 H. Said and R. Castanet, J. Less-Common Met., 68 (1979) 213.
24 M.V. Plotnikov, E.A. Aleshina, A.V. Makarov and V.P. Zlomanov, Inorg. Mater. (USSR), 19 (1983) 1160.
25 R. Hultgren, P.D. Desai, D.T. Hawkins, N. Gleiser, K.K. Kelly and D.D. Wagman, Selected Values of the Thermodynamic Properties of the Elements, American Chemical Society for Metals, Metals Park, OH 44073, USA, 1973.
26 S.A. Myers and D.H. Tracy, Spectrochim. Acta, Part B, 38 (1983) 1227.
27 J.G. Edwards, Nat. Bur. Stand. (U.S.), Spec. Publ., 561 (1979) 67.
28 J.G. Edwards and R.D. Freeman, High Temp. Sci., 12 (1980) 197.
29 J.K.R. Weber and J.G. Edwards, High Temp. Sci., 28 (1990) 175.
30 A.S. Gates and J.G. Edwards, J. Phys. Chem., 82 (1978) 2789.
31 J.G. Edwards and S.T. Kshirsagar, Thermochim. Acta, 59 (1982) 81.
32 J.G. Edwards and H.B. Thompson, Thermochim. Acta, 132 (1988) 67.
33 J.G. Edwards, D. Ferro and J.K.R. Weber, J. Less-Common Met., 156 (1989) 369.
34 C.E. Cater in R.A. Rapp (Ed.), Technique of Metals Research, Vol. IV, Part I, Wiley, New York, 1970, Chapter 2A.
35 P. Kapias and J.G. Edwards, J. Phys. Chem., 92 (1988) 3649.
36 R.S. Srivinasa and J.E. Edwards, J. Electrochem. Soc., 134 (1987) 1811.
37 G.N. Lewis and M. Randal, Thermodynamics, revised by K.S. Pitzer and L. Brewer, McGraw-Hill, New York, 1961, pp. 57 and 517.
38 R. Castanet and C. Bergman, J. Chem. Thermodyn., 9 (1977) 1127.
39 S. Takeda, S. Tamaki, A. Takano and H. Okazaki, J. Phys. C, 16 (1983) 467.
40 M.W. Chase, Jr., C.A. Davies, J.R. Downey, Jr., D.J. Frurip, R.A. McDonald and A.N. Syverud, J. Phys. Chem. Ref. Data, Suppl. 1, 14 (1985).
41 V.I. Belousov, N.F. Vendrikh, S.I. Gorbov, A.F. Novozhilov and A.S. Pashinkin, Inorg. Mater. (USSR), 20 (1984) 1135.

APPENDIX A: DERIVATION OF THE EQUATION FOR THE MOLE FRACTION OF THE VAPOR SPECIES

The system is taken to be made of two components: A (Te_2) and B (Ga_2Te); the molecular weights of A(g) (255), B(g) (267), and the Knudsen average molecular weight [37] of effusing species (264) are taken to be the same.

From the effusion cell, the rate of mass loss of A, $\dot{g}_A$, is

$$\dot{g}_A = \frac{dg_A}{dt} = P_A E \sqrt{\frac{M_A}{2\pi RT}} \tag{A1}$$

where P_A is partial pressure of A, E is effective orifice area, and M_A is the molecular weight of A. During the effusion period, τ, the mass of A in the condensed phase is

$$g_A^s(\tau) = g_A^s(0) - \int_0^\tau \dot{g}_A \, dt \tag{A2}$$

$$= g_A^s(0) - \int_0^\tau P X_A^v E \sqrt{\frac{M_A}{2\pi RT}} \, dt \tag{A3}$$

where $g_A^s(0)$, X_A^v, and P are the original mass of A in the condensed phase, the mole fraction of A in the vapor, and the total pressure, respectively. The number of moles of A in the condensed phase is

$$n_A^s(\tau) = n_A^s(0) - \int_0^\tau \frac{P X_A^v E}{\sqrt{2\pi RTM_A}} \, dt \tag{A4}$$

Let us assume that during time τ the composition of A in the vapor is constant. Such an assumption would be valid during an isothermal univariant vaporization.

$$n_A^s(\tau) = n_A^s(0) - \frac{PEX_A^v \tau}{\sqrt{2\pi RTM_A}} \tag{A5}$$

$$= n_A^s(0) - C_A \tau \tag{A6}$$

where

$$C_A = \frac{PEX_A^v}{\sqrt{2\pi RTM_A}} \tag{A7}$$

An equation equivalent to eqn. (A6) follows for component B.

The mole fraction of A in the condensed phase is

$$X_A^s(\tau) = \frac{n_A^s(0) - C_A \tau}{n_A^s(0) + n_B^s(0) - (C_A + C_B)\tau} \tag{A8}$$

From the Knudsen equation, the time τ and the mass loss, Δg^v, are

related by

$$\tau = \frac{\Delta g^{v}(\tau)\sqrt{\frac{2\pi RT}{M}}}{PE} \tag{A9}$$

By multiplication of eqn. (A7) by eqn. (A9), we obtain

$$C_A \tau = \frac{X_A^v \Delta g^v(\tau)}{M} \tag{A10}$$

Because of the assumption of equal molecular weights of A and B, the mole fraction of A in the condensed phase is given by

$$X_A^s(0) = \frac{g_A^s(0)}{g^s(0)} \tag{A11}$$

and the fraction of mass loss at time τ is given by

$$f(\tau) = \frac{\Delta g^v(\tau)}{g^s(0)} \tag{A12}$$

Upon substitution of $g_A^s(0)$ from eqn. (A11) into eqn. (A8), we obtain the mole fraction of A in the condensed phase to be

$$X_A^s(\tau) = \frac{g_A^s(0) - X_A^v(\tau)\,\Delta g^v(\tau)}{g^s(0) - \Delta g^v(\tau)} \tag{A13}$$

Upon substitution of $\Delta g^v(\tau)$ from eqn. (A12) into eqn. (A13), we obtain the mole fraction of A in the condensed phase to be

$$X_A^v(\tau) = \frac{x_A^s(0) - X_A^v f(\tau)}{1 - f(\tau)} \tag{A14}$$

and the mole fraction of A in the vapor phase to be

$$X_A^s(\tau) = \frac{X_A^s(0) - [1 - f(\tau)]X_A^s(\tau)}{f(\tau)} \tag{A15}$$

To determine the composition of the vapor, the starting and final compositions of the solid at any fraction of mass loss must be known, and compositions must be expressed in terms of X_{Te_2} instead of X_{Te}. The two parameters are related by

$$X_{Te_2} = \frac{3X_{Te} - 1}{1 + X_{Te}} \tag{A16}$$

As X_{Te_2} approaches 0, X_{Te} approaches 0.333, the fraction of Te in Ga_2Te. Uncertainties in X_{Te_2} are propagated from those in X_{Te}.

APPENDIX B: DATA IN SETS 1-4

TABLE B1

Temperature, vapor pressures, percentage mass loss, and apparent molecular weight from Set 1 with Cell TC1

Order	Group	T (K)	P_v (Pa)	P_k (Pa)	App. MW	Mass loss (%)
1	1	921	0.54	0.54	264	0.5
2	1	963	0.10	0.08	169	1.1
3	2	1085	3.00	2.97	259	4.8
4	2	1045	0.65	0.57	203	5.5
5	2	1017	0.22	0.21	241	5.9
6	2	1043	0.38	0.33	199	6.8
7	2	1081	1.61	1.45	214	8.1
8	2	1045	0.43	0.37	196	8.5
9	2	1091	2.18	2.00	222	10.2
10	2	971	0.03	0.03	264	10.3
11	3a	1065	0.81	0.70	197	11.0
12	3b	1019	0.17	0.16	234	11.6
13	3a	1040	0.40	0.35	202	12.7
14	3a	1059	0.68	0.59	199	14.1
15	3b	1000	0.09	0.07	160	14.2
16	3b	1027	0.24	0.21	202	14.6
17	3b	983	0.04	0.04	264	14.8
18	3a	1033	0.25	0.25	264	15.3
19	3b	985	0.05	0.05	264	15.4
20	3a	1066	0.83	0.76	221	16.4
21	3a	1045	0.37	0.37	264	17.2
22	3b	1017	–	0.15	–	17.7
23	3a	1071	1.02	–	–	18.8
24	3a	1059	0.71	0.64	215	19.6
25	3b	1006	0.10	0.08	169	19.7
26	3b	1029	0.21	0.20	239	20.7
27	3b	1007	0.10	0.09	214	21.2
28	3a	1039	0.31	0.30	247	21.6
29	3b	1022	0.16	0.16	264	22.3
30	3a	1065	0.77	0.74	244	23.5
31	3a	1088	1.90	1.77	229	25.3
32	3a	1062	0.67	0.60	212	27.0
33	3b	998	0.08	–	–	27.2
34	3a	1056	0.57	0.51	211	27.9
35	3a	1088	1.84	1.68	220	33.2
36	3b	1019	0.17	0.14	179	33.6
37	3a	1078	1.30	1.16	210	36.7
38	3b	1026	0.21	0.18	194	37.1
39	3b	988	0.06	0.04	117[a]	37.3
40	3a	1049	0.44	0.37	187	38.1
41	3b	1004	0.09	0.09	264	38.3
42	3b	998	0.08	0.06	149	38.5
43	3a	1075	1.08	0.98	217	40.4

TABLE B1 (continued)

Order	Group	T (K)	P_v (Pa)	P_K (Pa)	App. MW	Mass loss (%)
44	3b	1021	0.17	0.15	206	40.7
45	3a	1043	0.34	0.34	264	41.4
46	3b	1011	0.11	0.10	218	41.7
47	3a	1052	0.37	0.32	197	44.3
48	3a	1069	0.88	0.80	218	49.8
49	3a	1101	2.79	2.57	224	52.3
50	3a	1076	1.01	0.90	210	58.6
51	3a	1059	0.62	0.54	200	59.7
52	3b	1000	0.09	0.07	160	60.1
53	3a	1050	0.45	0.40	209	61.1
54	3a	1098	2.24	2.01	213	62.8
55	3a	1055	0.52	0.46	207	63.8
56	3a	1082	1.31	1.21	225	68.8
57	3b	1001	0.08	0.08	264	69.1
58	3b	1024	0.18	0.15	183	69.4
59	3a	1039	0.31	0.29	231	73.6
60	3a	1036	0.27	0.23	192	74.3
61	3a	1083	1.39	1.27	220	76.8
62	3a	1088	1.48	1.35	220	79.2
63	3a	1051	0.45	0.42	230	80.4
64	4b	1029	0.20	0.18	214	80.9
65	4a	1072	0.85	0.80	234	84.3
66	4b	1023	0.17	–	–	84.5
67	4b	1013	0.12	0.11	222	84.6
68	4a	1088	1.28	1.14	209	85.7
69	4b	1010	0.11	0.08	140	86.3
70	4a	1086	1.04	0.95	220	88.3
71	4a	1047	0.40	0.35	202	89.3
72	4b	989	0.05	0.05	264	89.5
73	4a	1067	0.66	0.58	204	90.1
74	4b	1019	0.15	0.14	230	90.6
75	4a	1078	0.85	0.79	228	91.7
76	4a	1052	0.44	0.38	197	92.2
77	4b	1014	0.13	0.12	225	92.5
78	4a	1094	1.21	1.06	203	93.2
79	4a	1064	0.57	0.49	195	94.0
80	4a	1083	0.89	0.80	213	94.6
81	4a	1067	0.51	0.47	224	95.4
82	4a	1041	0.28	0.25	210	95.8
83	5	1094	0.46	0.50	312	96.8
84	5	1053	0.15	0.19	424	97.2
85	5	1069	0.14	0.15	303	97.5
86	5	1085	0.02	0.02	264	97.7

[a] Value excluded on statistical basis.

TABLE B2

Temperature, vapor pressures, percentage mass loss, and apparent molecular weight from Set 2 with Cell TC2

Order	Group	T (K)	P_v (Pa)	P_K (Pa)	App. MW	Mass loss (%)
1	1	929	0.53	0.57	305	0.2
2	1	1011	0.28	0.63	1,336 [a]	1.8
3	2	1033	0.50	0.44	204	2.0
4	2	1084	2.66	2.28	194	5.2
5	2	1066	1.73	1.34	158	6.4
6	2	1056	1.00	0.92	223	6.7
7	2	1030	0.38	0.34	211	6.9
8	2	1077	2.03	1.78	203	8.2
9	2	1086	2.21	1.81	177	10.1
10	3b	1009	0.12	0.10	183	10.2
11	3b	1020	0.14	0.15	303	10.3
12	3a	1093	1.45	1.35	229	12.4
13	3a	1077	0.65	0.64	256	12.7
14	3a	1098	1.86	1.71	223	14.0
15	3a	1064	0.63	0.46	141	14.3
16	3b	1030	0.33	0.14	48 [a]	14.4
17	3a	1048	0.28	0.27	245	14.6
18	3a	1075	0.71	0.62	201	15.2
19	3a	1089	1.29	1.12	199	15.7
20	3b	1009	0.06	0.04	117 [a]	15.9
21	3a	1079	0.89	0.71	168	17.1
22	3a	1078	0.84	0.80	239	17.5
23	3a	1046	0.32	0.26	174	17.7
24	3a	1093	1.50	1.29	195	18.6
25	3a	1081	1.12	0.86	156	20.3
26	3a	1041	0.21	0.21	264	20.4
27	3a	1082	0.93	0.84	215	21.1
28	3b	1001	0.05	–	–	21.1
29	3a	1033	0.16	0.16	264	21.2
30	3a	1080	1.06	0.84	166	22.8
31	3a	1086	1.13	1.02	215	23.9
32	3a	1086	1.22	0.98	170	24.5
33	3a	1087	1.24	1.02	179	27.1
34	3a	1077	0.80	0.66	180	28.2
35	3a	1080	1.03	0.76	144	30.1
36	3a	1050	0.28	0.25	210	30.3
37	3b	1011	0.10	–	–	30.4
38	3a	1032	0.18	–	–	30.4
39	3a	1065	0.53	0.43	174	30.6
40	3a	1075	0.85	0.64	150	32.1
41	3a	1070	0.63	0.55	201	32.7
42	3a	1038	0.27	0.17	105 [a]	32.8
43	3a	1073	0.77	0.60	160	34.0
44	3a	1058	0.38	0.38	264	34.2
45	3b	1016	0.10	–	–	34.2

TABLE B2 (continued)

Order	Group	T (K)	P_V (Pa)	P_K (Pa)	App. MW	Mass loss (%)
46	3a	1053	0.38	0.32	187	34.5
47	3a	1082	1.03	0.84	176	36.2
48	3a	1065	0.54	0.53	254	36.5
49	3b	1007	0.09	–	–	36.5
50	3a	1044	0.30	0.23	155	36.7
51	3a	1091	1.37	1.19	199	37.6
52	3a	1074	0.80	0.69	196	38.4
53	3a	1033	0.18	0.18	264	38.6
54	3a	1060	0.47	–	–	38.8
55	3b	1028	0.21	–	–	38.9
56	3a	1084	1.14	0.98	195	40.5
57	3b	1017	0.10	0.09	214	40.5
58	3b	996	0.06	–	–	40.5
59	3b	1017	0.11	–	–	40.6
60	3a	1070	0.68	0.54	166	41.8
61	3a	1079	0.91	0.76	184	43.5
62	3a	1079	0.91	0.74	175	45.3
63	3a	1032	0.25	0.15	95 [a]	46.2
64	3b	1026	0.22	–	–	46.3
65	3a	1068	0.63	0.50	166	47.0
66	3a	1051	0.34	0.31	219	47.2
67	3a	1036	0.22	0.17	158	47.3
68	3a	1045	0.32	0.23	136	47.7
69	3a	1081	0.97	0.85	203	48.7
70	3a	1046	0.32	0.25	161	49.5
71	3b	1019	0.14	0.10	135	49.6
72	3b	1028	0.20	0.14	129	50.3
73	3b	1017	0.16	–	–	50.3
74	3a	1085	1.13	0.97	195	50.7
75	3a	1074	0.77	0.64	182	52.2
76	3b	999	0.10	–	–	52.4
77	3a	1080	0.96	0.85	207	53.7
78	3b	1007	0.06	–	–	53.8
79	3a	1054	0.39	0.34	201	54.2
80	3b	1011	0.10	–	–	54.2
81	3a	1079	0.93	0.82	205	56.1
82	3a	1048	0.28	0.28	264	56.3
83	3a	1058	0.44	0.39	207	56.6
84	3a	1094	1.54	1.44	231	57.9
85	3a	1079	0.84	0.74	205	59.1
86	3b	1009	0.07	–	–	59.3
87	3a	1088	1.30	1.16	210	61.4
88	3a	1068	0.58	0.52	212	62.5
89	3a	1031	0.12	–	–	62.6
90	3a	1057	0.39	0.38	251	63.4
91	3a	1092	1.39	1.37	256	64.2
92	3b	1025	0.15	–	–	64.3
93	3a	1041	0.25	0.21	186	64.4

TABLE B2 (continued)

Order	Group	T (K)	P_V (Pa)	P_K (Pa)	App. MW	Mass loss (%)
94	3a	1097	1.71	1.65	246	65.3
95	3b	993	0.04	–	–	65.3
96	3a	1096	1.69	1.56	225	65.9
97	3b	1029	0.20	0.16	169	66.0
98	3a	1100	2.07	1.92	227	67.3
99	3a	1069	0.70	0.58	181	68.6
100	3b	1013	0.10	–	–	68.8
101	3a	1069	0.71	0.62	201	69.4
102	3a	1041	0.31	0.23	145	69.5
103	3a	1094	1.60	1.44	214	70.3
104	3b	1005	0.15	–	–	70.3
105	3b	1001	0.06	–	–	70.3

[a] Value excluded on statistical basis.

TABLE B3

Temperature, vapor pressures, percentage mass loss, and apparent molecular weight from Set 3 with Cell TC3

Order	Group	T (K)	P_V (Pa)	P_K (Pa)	App. MW	Mass loss (%)
1	1	970	3.34	3.70	324	2.1
2	1	950	1.34	1.60	376	2.6
3	2	1041	1.59	1.23	158	4.0
4	2	1076	4.06	3.63	211	5.3
5	2	1064	2.63	2.54	246	6.0
6	2	1002	0.34	0.33	249	6.3
7	2	1041	1.17	1.19	273	6.8
8	2	1061	2.35	2.34	262	8.2
9	2	1005	0.31	0.28	215	8.4
10	2	1074	3.67	3.61	255	9.6
11	2	1068	2.99	2.93	253	10.7
12	2	1048	1.61	1.36	188	11.1
13	2	1018	0.55	0.56	274	13.5
14	2	1083	4.48	4.56	274	15.7
15	2	1040	1.11	1.01	219	16.5
16	2	1071	3.24	3.13	246	17.6
17	2	1063	2.46	2.29	229	18.5
18	2	1049	1.56	–	–	20.0
19	2	1054	1.73	1.47	191	20.2
20	2	1089	4.95	4.61	229	22.5
21	2	1041	1.17	0.94		23.6
22	3a	1064	1.39	1.23	207	24.9
23	3b	1021	0.29	0.29	264	25.0
24	3a	1090	2.68	2.43	217	25.6
25	3a	1046	0.60	0.49	176	25.8
26	3a	1086	2.16	2.09	247	27.0

TABLE B3 (continued)

Order	Group	T (K)	P_v (Pa)	P_K (Pa)	App. MW	Mass loss (%)
27	3b	1005	0.32	–	–	28.5
28	3b	1007	0.12	–	–	28.6
29	3a	1096	3.07	3.14	276	29.7
30	3a	1075	1.35	1.26	230	30.1
31	3a	1049	0.59	0.56	238	30.4
32	3b	986	0.08	–	–	30.5
33	3b	974	0.03	–	–	32.4
34	3a	1088	2.16	2.18	269	33.1
35	3a	1076	1.34	1.24	226	33.6
36	3a	1049	0.64	0.66	281	34.3
37	3a	1078	1.59	1.59	264	36.6
38	3a	1089	3.24	3.10	242	37.2
39	3a	1041	0.48	0.42	202	37.4
40	3a	1074	1.24	1.17	235	37.7
41	3a	1077	1.36	1.33	252	40.9
42	3b	994	0.07	–	–	41.0
43	3a	1091	2.28	2.38	289	42.5
44	3a	1041	0.44	0.42	241	42.6
45	3b	998	0.08	–	–	42.6
46	3a	1073	1.11	1.16	288	42.8
47	3b	995	0.09	0.08	209	44.4
48	3a	1065	0.93	0.89	242	44.5
49	3a	1052	0.62	0.58	231	44.8
50	3a	1091	2.20	2.18	259	45.4
51	3a	1035	0.42	0.30	135	45.5
52	3a	1095	2.75	2.68	251	46.3
53	3a	1075	1.23	1.21	255	48.9
54	3a	1099	3.01	3.07	275	49.8
55	3a	1081	1.64	1.56	239	50.4
56	3b	1011	0.27	0.14	71 [a]	50.5
57	3a	1035	0.45	0.32	134	50.8
58	3b	1026	0.26	0.25	244	52.1
59	3a	1051	0.58	0.56	246	52.3
60	3a	1085	1.74	1.76	270	53.0
61	3b	1025	0.31	0.23	145	53.1
62	3a	1100	3.26	3.24	261	54.4
63	3a	1080	1.42	1.41	260	56.9
64	3b	1020	0.21	0.20	239	57.1
65	3a	1098	3.01	2.86	238	58.6
66	3a	1048	0.56	0.48	194	59.5
67	3a	1052	0.63	0.56	209	60.1
68	3a	1059	0.97	0.93	243	64.3
69	3a	1050	0.54	0.49	217	65.5
70	3a	1075	1.33	1.23	226	65.6

[a] Value excluded on statistical basis.

TABLE B4

Temperature, vapor pressures, percentage mass loss, and apparent molecular weight from Set 4 with Cell TC3

Order	Group	T (K)	P_V (Pa)	P_K (Pa)	App. MW	Mass loss (%)
1	1	1056	3.35	3.06	220	0.5
2	1	1021	1.12	1.09	250	1.5
3	1	998	0.48	0.50	286	1.6
4	3a	1046	0.64	0.59	224	2.2
5	3a	1073	1.47	1.38	233	2.5
6	3a	1056	0.88	0.84	241	3.2
7	3a	1053	0.79	0.77	252	3.4
8	3a	1038	0.49	0.43	203	3.6
9	3a	1063	1.05	1.05	264	4.7
10	3a	1075	1.66	1.59	242	4.9
11	3a	1076	1.62	1.59	254	5.2
12	3a	1046	0.61	0.57	231	5.5
13	3b	1020	0.28	0.23	178	5.6
14	3a	1081	1.89	1.89	264	6.4
15	3a	1083	2.08	1.98	239	7.8
16	3b	1010	0.16	0.17	298	8.1
17	3a	1081	1.81	1.74	244	8.7
18	3a	1045	0.61	0.54	207	9.6
19	3a	1066	1.16	1.06	220	10.0
20	3b	1007	0.17	0.16	234	10.9
21	3a	1077	1.56	1.50	244	12.2
22	3b	1029	0.38	0.30	165	12.7
23	3a	1088	2.18	2.19	266	14.7
24	3a	1034	0.36	0.36	264	15.0
25	3a	1086	1.96	1.92	253	15.6
26	3a	1102	3.73	3.64	251	17.6
27	3b	1023	0.38	0.23	97 [a]	18.7
28	3a	1046	0.50	0.48	243	19.8
29	3a	1087	2.12	2.22	290	21.4
30	3a	1040	0.51	0.43	188	21.5
31	3a	1067	1.18	1.06	213	23.0
32	3a	1096	2.99	3.08	280	24.2
33	3b	1024	0.32	0.28	202	24.3
34	3a	1093	2.68	2.53	235	25.8
35	3b	1030	0.45	0.35	160	26.0
36	3a	1045	0.51	–	–	27.6
37	3a	1043	0.46	0.43	231	27.7
38	3a	1101	3.65	3.36	224	28.4
39	3a	1052	0.64	0.60	232	28.6
40	3a	1078	1.58	1.57	261	29.2
41	3a	1081	1.68	1.53	219	31.8
42	3b	1025	0.24	0.22	222	32.0
43	3a	1098	3.13	2.99	241	32.7
44	3b	1014	0.23	0.17	144	32.9
45	3a	1090	2.35	2.25	242	33.5

TABLE B4 (continued)

Order	Group	T (K)	P_v (Pa)	P_K (Pa)	App. MW	Mass loss (%)
46	3a	1095	2.71	2.68	258	34.7
47	3b	1029	0.36	0.30	183	35.1
48	3a	1101	3.34	3.22	245	35.7
49	3a	1059	0.87	0.85	252	39.0
50	3a	1082	1.86	1.81	250	39.5
51	3a	1086	1.92	1.97	278	40.1
52	3a	1069	1.30	1.21	229	43.4
53	3a	1064	0.94	0.93	258	43.8
54	3a	1059	0.74	0.70	236	43.9
55	3a	1095	2.46	2.31	233	44.8
56	3a	1101	2.72	2.68	256	45.3
57	3b	1021	0.35	0.25	135	45.4
58	3a	1092	2.11	2.06	252	46.1
59	3a	1077	1.38	1.40	272	46.4
60	3a	1097	2.38	2.28	242	47.9
61	3a	1035	0.48	0.37	157	48.2
62	3a	1102	2.44	2.37	249	52.3
63	3a	1046	0.63	0.52	180	52.5
64	3a	1093	1.97	1.93	253	53.9
65	3a	1098	2.09	2.08	261	54.9
66	3a	1053	0.76	0.64	187	55.4
67	3a	1099	2.01	1.99	259	56.9
68	3b	1030	0.43	0.29	120 [a]	57.0
69	3a	1068	1.04	0.90	198	57.6
70	3b	1023	0.22	0.23	289	59.7
71	3a	1093	1.70	1.64	246	60.2
72	3a	1058	0.74	0.69	230	60.4
73	3a	1079	1.23	1.16	235	61.2
74	3a	1036	0.44	0.38	197	61.3
75	3a	1089	1.55	1.44	228	62.3
76	3a	1052	0.70	0.55	163	62.4
77	3a	1098	2.01	1.88	231	62.9

[a] Value excluded on statistical basis.